Comprehensive modeling of ventilation systems for Nearly Zero Energy Buildings

Comprehensive modeling of ventilation systems for Nearly Zero Energy Buildings

R Sedoni[1,*], G Cannistraci[1], P E Santangelo[1,2], D Angeli[1,3], M Romani[4], L Fioravanti[4]

[1] DISMI - Dipartimento di Scienze e Metodi dell'Ingegneria, Università degli studi di Modena e Reggio Emilia, Reggio Emilia (Italy)
[2] Centro interdipartimentale per la ricerca InterMech – MO.RE., Modena (Italy)
[3] Centro Interdipartimentale En&Tech, Reggio Emilia (Italy)
[4] Zehnder Group – Competence Center Campogalliano, Campogalliano (Italy)

* Corresponding author: 225791@studenti.unimore.it

Abstract. In the present work, a lumped-parameter model of a multifunctional ventilation unit for residential applications was developed in the Simulink environment, also relying on the Simscape toolbox with Moist Air and Two-Phase fluid libraries. A simple, yet effective method to analyze and optimize the efficiency of the combined HVAC – air distribution system is proposed. To investigate the impact of boundary conditions on system performance, a parametric study of different installation conditions was also carried out, including outdoor air and indoor air temperature, humidity, static pressure, filter fouling, pressure drop in the intake and distribution ducts. The model highlights a strong decrease in the useful cooling/heating heat flow rate produced by the system as the installation and maintenance conditions become more challenging.

Keywords: lumped-parameter model, multifunctional ventilation unit, moisture transport, ventilation mode, filter

1. Introduction

Nowadays HVAC systems play a crucial role in maintaining indoor air quality, thermal comfort, and energy efficiency in buildings. With the increasing focus on sustainability and energy efficiency, there is a growing need to improve HVAC systems and their operation. HVAC systems consume a significant amount of energy in buildings, and their inefficient operation can result in wasted energy, increased carbon emissions, and increased energy costs [1]. Therefore, improving the efficiency of HVAC systems has become an important research topic.

In the past, numerous efforts have been made by researchers for the development of simple analytical models to study some fundamental components of air treatment systems, including the most important one: the enthalpy recovery exchanger [2,3], and the diffusivity characteristics of its permeable membrane [4, 5].

Studies have also been conducted to analyze the effect of specific boundary conditions on the performance of standard ventilation units. Manz et al. [6] investigated the performance of a single room ventilation unit with recuperative or regenerative heat recovery exchangers. Filis

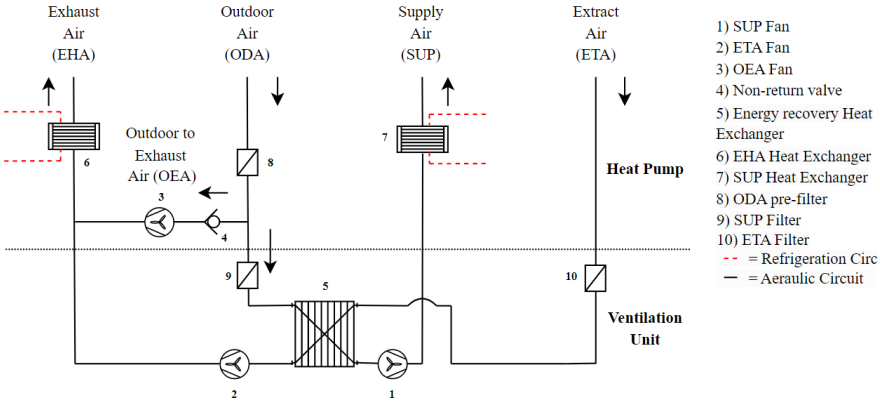

Figure 1. Full schematic of the HVAC unit investigated

et al. [7] investigated the effects of wind pressure and stack effect on total sensible heat recovery and supply air temperatures when using different fan types, airflow rates, and fan operating points.

This paper presents a comprehensive analysis of an innovative HVAC commercial unit for nZEB buildings, using a simple approach that can take into account all the possible effects to which the system may be subjected. For this purpose a new Simscape block for the Moist Air library was developed to model the enthalpy heat exchangers. The study specifically focuses on the critical aspects linked to the inclusion of an additional fan aimed at improving the unit performance.

2. System description

The system under consideration combines a balanced mass/volume flow ventilation unit with an air-to-air heat pump to optimize energy consumption and provide thermal comfort in residential buildings. This system works differently from standard products, in that the ventilation unit operates at a flow rate ranging between 0 and 450 m^3h^{-1}, while the heat pump unit operates with a balanced mass/volume flow rate ranging between 0 and 600 m^3h^{-1}, thanks to the contribution of a third fan (OEA) in the heat pump unit. Outdoor air (ODA) is extracted from the environment by the ventilation unit fan, and then conveyed through the heat pump ducts, preheater, energy recovery ventilation (ERV) or heat recovery ventilation (HRV) heat exchanger, and the evaporator or condenser heat exchanger of the heat pump. The resulting supply air (SUP) mass/volume flow is then delivered to the building where the system is installed. Another part of the circuit deals with extracted air (ETA) from the internal environment, which is discharged to the outdoor, called exhaust air (EHA), after passing through the ERV or HRV and heat exchanger of the HP. To increase the heat transfer rate at the evaporator (in heating mode) or condenser (in cooling mode), a third fan has been introduced in the heat pump. This fan draws air from the environment through the supply duct and drives it directly into the EHA duct upstream of the heat exchanger through a bypass line, thus increasing the EHA mass/volume flow rate. It is important to note that the OEA fan has specific operating limits, such as a maximum revolution speed of 2500 rpm, and a limited dimension. These limits were implemented to meet the design requirement of reducing and controlling noise levels, ultimately ensuring the acoustic comfort of the occupants. A full schematic view of the aeraulic circuit system is shown in Figure 1.

3. Model development

3.1. Aeraulic circuit

Regarding the aeraulic side of the circuit, the pressure drops of the individual components that make up the circuit (such as air ducts, filters, check valve, ERV/HRV, and T-junctions) are calculated using the known relationship:

$$\Delta p = R\dot{m}^2 \tag{1}$$

Where R is the specific resistance of the component, and $\dot{m}$ is the mass flow through the component. The values of R are commonly obtained from the technical data sheets of individual components. The 'Fan (MA)' [8] block is used to model the fans operating curves and the 'Condenser-Evaporator (2P-MA)' [8] block is used to model the two exchangers of the heat pump (EHA and SUP).

3.2. ERV/HRV modeling

ERV/HRV heat exchangers typically consist of a series of rectangular channels that primarily operate in counterflow. However, there is a small portion of the exchanger in cross-flow configuration. Despite of this portion, considering only the counterflow part of the heat exchanger for determining the exchange characteristics does not lead to a significant error.

A pre-defined type of heat exchanger similar to this one, currently, is not available in Simscape, so it was necessary to reconstruct it starting from the base block, i.e. 'Pipe (MA)' [8].

To simplify the modeling process, the overall heat transfer characteristics of the exchanger are determined based on a single channel (fig. 2) using a counterflow model approach and then extrapolated to the entire heat exchanger. The positive heat and moisture transfer direction is assumed from the ETA to the SUP side (control volume 3 to 1).

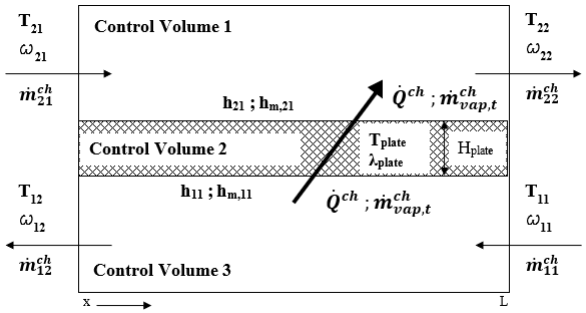

Figure 2. Counterflow model approach

3.2.1. Sensible Load Regarding the sensible heat recovered in the exchanger, the effectiveness-NTU method has been implemented. The equations for the sensible heat recovery are derived from the available literature [2].

The thermal power exchanged between two channels ($\dot{Q}^{ch}$) is:

$$\dot{Q}^{ch} = \epsilon_s \dot{Q}^{ch}_{max} = \epsilon_s (\dot{m}^{ch} cp)_{min} (T_{11} - T_{21}) \qquad \epsilon_s = \frac{1 - e^{-NTU_s(1-C_r)}}{1 - C_r e^{-NTU_s(1-C_r)}} \tag{2}$$

Where ϵ_s is the sensible effectiveness for a counterflow exchanger, T_{11} is the inlet ETA flow temperature, T_{21} is the inlet SUP flow temperature, $\dot{Q}^{ch}_{max}$ is the maximum recoverable heat flow rate per channel and $\dot{m}^{ch}_{11}$ and $\dot{m}^{ch}_{21}$ are the inlet mass flow rate per channel, on the ETA side and SUP side respectively.

Given the very small size of the channels, for this type of ERV/HRV exchanger, the flow is laminar (Re = 90÷ 110), so the relationship derived by Shah et al. [2] is used to calculate the Nusselt number in rectangular channel heat exchangers:

$$Nu = 8.235[1 - 2.0421(\alpha^*) + 3.0853(\alpha^*)^2 - 2.4765(\alpha^*)^3 + 1.0578(\alpha^*)^4 - 0.1861(\alpha^*)^5] \quad (3)$$

Where α^* is the ratio between the two dimensions (a,b) of the channel cross-section. For a square channel $\alpha^* = \frac{a}{b} = 1$ and therefore Nu = 3.608.

Multiplying by the total number of channels per side ($n_{channel}$), it is possible to calculate the overall heat exchange in the ERV/HRV ($\dot{Q}$):

$$\dot{Q} = n_{channel}\dot{Q}^{ch} \quad (4)$$

To simulate the thermal inertia of the heat exchanger membrane and thus obtain a more accurate modeling of thermal exchange during transients, a thermal mass has also been introduced in the model.

3.2.2. Latent load For an ERV-type heat recovery system, it is necessary to introduce an amount of recovered moisture. The equations for moisture recovery are derived mainly from the work of Križo et al. [4] , Min et al. [5] and Zhang et al. [9].

In a similar fashion to equation (2) it is possible to define the amount of moisture transferred between two channels ($\dot{m}^{ch}_{vap,t}$) as:

$$\dot{m}^{ch}_{vap,t} = \epsilon_l(\dot{m}^{ch}_{dry})_{min}(\omega_{11} - \omega_{21}) \quad (5)$$

Where $\dot{m}^{ch}_{dry}$ is the mass flow rate of dry air per channel, and ω_{11} and ω_{21} are the humidity ratios of the two flows. So the latent effectiveness (ϵ_l) can be calculated as:

$$\epsilon_l = \frac{1 - e^{-NTU_l(1-R)}}{1 - Re^{-NTU_l(1-R)}} \qquad R = \frac{\dot{m}^{ch}_{min}}{\dot{m}^{ch}_{max}} \qquad NTU_l = \frac{U_l A^{ch}}{\dot{m}^{ch}_{min}} \quad (6)$$

The total moisture transfer resistance (U_l) is:

$$U_l = \left(\frac{1}{h_{m,11}} + \frac{H_{plate}}{P_m} + \frac{1}{h_{m,21}}\right)^{-1} \qquad P_m = \frac{CD_{wm}\omega_{max}e^{5294/T}}{10^6(1 - C + \frac{C}{RH})^2RH^2} \quad (7)$$

Where H_{plate} is the thickness of the membrane, P_m is the membrane permeability, D_{wm} is the moisture diffusivity in membrane, ω_{max} represents the maximum moisture content of the water vapor in the membrane and C gives the shape of the sorption curve. For simplicity, these properties were assumed to be constant in the model, and the values at 20°C were used, allowing for a small error. Temperature T and relative humidity RH in equation (8) are chosen as the average values on the plate surface. The convective moisture transfer coefficient h_m can be obtained using the Chilton–Colburn analogy from the convective heat transfer coefficient, the Lewis number (Le is around 1.15 for air) [3], and from ρ and c_p of the air flow:

$$h_m = \frac{h}{\mathrm{Le}^{2/3}\rho c_p} \quad (8)$$

Finally the total transferred moisture is:

$$\dot{m}_{vap,t} = n_{channel}\dot{m}^{ch}_{vap,t} \quad (9)$$

Table 1. Experimental vs Model data

$\dot{m}$	$\epsilon_{sensible}$			ϵ_{latent}		
[kg/s]	**Experimental**	**Model**	**Error [%]**	**Experimental**	**Model**	**Error [%]**
0.0155	0.968	0.97	0.21	0.943	0.933	-1.06
0.1002	0.814	0.836	2.70	0.666	0.68	2.10
0.1417	0.779	0.782	0.39	0.589	0.6	1.87

3.2.3. ERV/HRV Model Validation The experiments for validation were carried out with T_{ODA}=2°C, RH_{ODA}=82% and T_{ETA}=20°C, RH_{ETA}=61%:

Where experimental effectivenesses are calculated as:

$$\epsilon_s = \frac{(\dot{m}c_p)_{21}(T_{22} - T_{21})}{(\dot{m}c_p)_{min}(T_{11} - T_{21})} \qquad \epsilon_l = \frac{(\dot{m})_{21}(\omega_{22} - \omega_{21})}{(\dot{m})_{min}(\omega_{11} - \omega_{21})} \tag{10}$$

As shown in Table 1, since the error of the ERV/HRV model is contained within acceptable limits, it can be considered as validated.

3.3. Aeraulic model calibration

The aeraulic model is calibrated according to experimental results provided by a notified body, that tested the system in the past. Experimentally, a volumetric flow rate of 227 m^3h^{-1} was set for extraction and supply air, the pressure drops were fixed on the external ducts, and the rotation speeds of the three fans were measured.

Table 2. OEA Volume flow rate comparison (Model forecast vs Experimental data)

n Fan Model	**n Fan Experimental**	**Volume flow OEA Model**	**Volume flow OEA Experimental**	**Percentage Error**
[rpm]	**[rpm]**	**[m^3/h]**	**[m^3/h]**	**[%]**
1930	1770	13.7	13	5.4
2060	1900	24.4	27	-9.6
2277	2117	46	48	-4.2
2477	2317	66	67	-1.5
2660	2500	85.3	85	0.3

We opted for a calibration approach based on the correction of the fan characteristic curves instead of the resistances; this appeared as the most convenient approach, given the high number of flow resistances involved and, on the other hand, the low number of fans. In this case, a correction factor of 160 rpm for the OEA fan allows for a faithful replication of the behavior of the real system. Similarly, a correction factor of 245 rpm was determined for the ETA fan, and 116 rpm were added to the SUP fan. These offsets were introduced to compensate uncertainties in the system:

- The correction on the OEA fan takes into account the uncertainties of the ODA, OEA, and EHA branch flow resistances, such as the ODA filter, the check valve, and T-junctions.
- In a similar fashion the correction on the ETA and SUP fans takes into account the uncertainties on the flow resistances of the ETA and SUP branches, and also accounts for the uncertainties on the fans operating curves, due to the presence of a scroll around the fans, designed to increase their performance.

It is possible to observe (Table 2) that the error decreases rapidly as the flow rate increases. This is mainly due to the fact that the dimensionless operating curve, at the small flow rates processed by the fan, deviates significantly from the actual operating fan curve. In this case, measurements were taken with deliberately high pressure drops on the external channels, to see the effect of these on the third fan; therefore the flow rate is in most cases, really small.

However, under nominal operating conditions, the system works with much higher flow rates. Therefore, the system can be considered to be calibrated with satisfactory accuracy, given the relatively low error on the higher flow rates.

4. Results and discussion

4.1. Effect of installation conditions

The focus of this paper is on the ventilation system and its performance; however a simple model of the thermodynamic cycle of the heat pump and of the refrigeration circuit is defined to complete the physical modeling of the whole system and perform sensitivity analyses. The description of the refrigeration model is omitted for brevity.

In this section, we analyze the results of the model by assessing different installation conditions:

Table 3. Installation conditions

	Installation		
	Ideal	**Medium**	**Critical**
ETA, SUP ducts lenght DN160 [m]	15	15	15
ODA, EHA ducts lenght DN200 [m]	1	0	0
ODA, EHA ducts lenght DN160 [m]	0	4	6
ETA, SUP number of bends 45°	2	4	6
ODA, EHA number of bends 45°	2	4	6
ETA, SUP Specific Flow Resistence [Pa s^2/kg^2]	10434	11868	13302
ODA, EHA Specific Flow Resistence [Pa s^2/kg^2]	721	5828	8462

The analyses were carried out in the winter season with $T_{ODA} = 2°C$, $RH_{ODA} = 50\%$, and indoor conditions of $T_{ETA} = 20°C$, $RH_{ETA} = 50\%$, $n_{OEA} = 2500$ rpm, $\dot{m}_{ETA} = \dot{m}_{SUP} = 0.025$ kg s^{-1} (~ 75 m^3h^{-1}).

The supply mass flow rate was purposely set as very low, precisely because the main advantage of this three-fan system lies in being able to provide high heat transfer rates even when the user requires reduced flow rates.

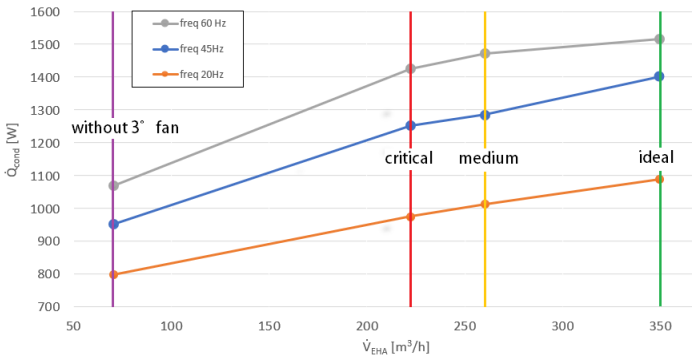

Figure 3. Condenser Heat transfer rate vs $\dot{V}_{EHA}$

For a compressor frequency of 45 Hz (fig. 3), it is observed that, for a constant supply flow rate, the presence of the OEA fan increases the heat transfer rate by 32% with respect to a traditional system in an ideal installation, owing to the increased flow rate at the evaporator. However, the heat transfer rate decreases as the external pressure drop on EHA and ODA channels increases, since the rotation velocity of the OEA fan is limited (due to noise) to 2500 rpm. Conversely, it has been ascertained that the impact of increasing external pressure losses

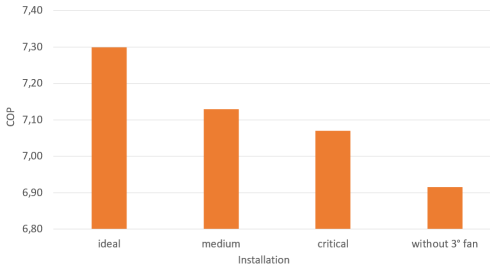

Figure 4. Variation of COP under different installations

on the ETA and SUP channels has an impact only on the ETA and SUP fans, which do not have limitations on their rotation velocity.

Finally, it can be observed from Figure 3 that the impact of reducing the available heat transfer rate to the condenser, as installation conditions vary, becomes increasingly severe at higher compressor frequencies.

An additional analysis that can be conducted is to study the influence of the OEA fan (and consequently, the installation) on the thermodynamic performance of the heat pump. In this case, the COP merely refers to the thermodynamic cycle.

The boundary conditions of the analysis under consideration are the same as in the previous case, apart from a supply flow rate of $\dot{m}_{ETA} = \dot{m}_{SUP} = 0.0752$ kg s^{-1} ($\sim$ 227 m^{3}h^{-1}). From Figure 4, a slight decrease in the COP is observed as installation conditions worsen.

To conclude the analysis, it is evident that the three-fan system presents significant advantages in terms of system performance. However, greater attention must be paid during the installation phase to ensure that these advantages are actually realized.

4.2. ODA Filter Fouling model (Maintenance)

The phenomenon of fouling within this work has been examined for the pre-filter located inside the ODA channel of the heat pump. This was done by evaluating the variation of system performance in terms of volumetric flow rate to the OEA fan, during the winter season (T_{ODA} = 2°C, RH_{ODA} = 50 %) for an ideal installation, with n_{OEA} = 2500 rpm. These analyses were carried out based on the following assumptions regarding fouling:

- The increase of pressure losses with time due to filter fouling is exponential [10].
- The maximum admissible value of pressure loss is three times the pressure loss of the clean filter [11].
- The considered period is 180 days from the installation of a new filter, after which fouling reaches the maximum admissible level.

A general pressure drop-fouling equation for the filter examined could then be defined:

$$\Delta p = R_{cleanfilter}(1 + e^{0.0294 \cdot d})\dot{m}^2 \tag{11}$$

Where d denotes the number of days past the installation, and $e^{0.0294 \cdot d}$ is the correction term accounting for filter fouling.

From the analysis of the data presented in Figure 5 (carried out with $\dot{V}_{SUP}$ = 227 m^{3}h^{-1}), it can be observed that, as time passes, the flow rate processed by the third fan in the heat pump (and consequently the heat transfer rate available at the evaporator) decreases by an amount which is not very high, but still significant if compared with the maximum expected

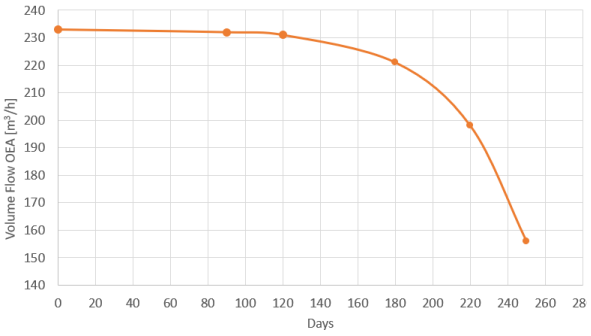

Figure 5. $\dot{V}_{OEA}$ fan degradation

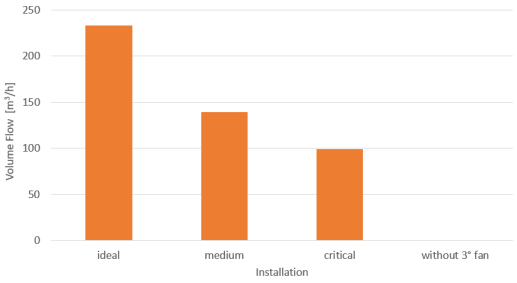

Figure 6. $\dot{V}_{OEA}$ vs Installation

performance. This behavior is due to the initial value of the filter pressure drop, which, being a large mesh filter, turns out to be quite small, even when triplicated at the 180th day.

After 180 days, the contribution of filter fouling begins to significantly degrade the system performance. For example, comparing Figure 6 and Figure 5, it can be observed that after 250 days the system behaves almost as if it were subjected to a medium installation, with all the consequences discussed in the previous section. It is therefore essential to respect the maximum 180-day interval between filter changes, as recommended by regulations, in order to always maintain acceptable system performance.

5. Conclusions

A comprehensive model of the air handling system of a ventilation machine coupled with a commercial heat pump has been successfully developed and experimentally calibrated. In particular, an ERV/HRV heat exchanger model was developed in Simscape and experimentally validated. A refrigeration circuit was then coupled to the system to show the effects of incorrect installation conditions, and thus the decay of the performance of the associated thermodynamic cycle.

6. References

[1] Dorer V and Breer D 1998 *Energy Build.* **27** 247–255
[2] Shah R K and Sekulic D P 2003 *Fundamentals of heat exchanger design* (John Wiley & Sons)
[3] Min J and Su M 2010 *Appl. Therm. Eng.* **30** 991–997
[4] Križo K, Kapjor A and Holubčík M 2022 *Energies* **15** 6021
[5] Min J, Hu T and Liu X 2010 *J. Membr. Sci.* **357** 185–191
[6] Manz H, Huber H, Schälin A, Weber A, Ferrazzini M and Studer M 2000 *Energy Build.* **31** 37–47
[7] Filis V, Kolarik J and Smith K M 2021 *Energy Build.* **234** 110689
[8] MathWorks URL `https://it.mathworks.com/help/simscape/physical-modeling.html`
[9] Zhang L Z, Liang C H and Pei L X 2008 *J. Membr. Sci.* **325** 672–682
[10] Eker O F, Camci F and Jennions I K 2016 *MSSP* **75** 395–412
[11] 2017 UNI EN ISO 16890-1:2017 Filtri d'aria per ventilazione generale Standard

Acknowledgement

We thank the Zehnder Group - Competence Center Campogalliano (MO) for the invaluable help throughout this research and for the resources made available to the purpose.